CHAPTER 5

STRENGTH REDUCTION METHOD FOR ANALYZING STABILITY OF TWO-LAYERED SOIL SLOPES

5.1 INTRODUCTION AND REVIEW OF EXISTING STUDIES

The aim of the present chapter is to utilize one of the widely used numerical approach called strength reduction method (SRM) for evaluating the stability of two-layered slopes. The primary focus is to provide a quantitative estimation of the improvement of slope stability when a stronger layer is placed over the weaker layer. The efficacy of variational formulation provided in the previous chapter is tested with the obtained numerical solutions. The SRM carried in this work comprises a series of finite element lower bound (LB) and upper bound (UB) limit analysis in conjunction with nonlinear optimization. The work of Zienkiewicz et al. (1975) appears to be the first where SRM was used to solve the slope stability problem. Following his work, many further studies (Naylor 1981; Matsui and San 1992; Griffiths and Lane 1999; Dawson et al. 1999; Lechman and Griffiths 2000; Zhao et al. 2005; Liu et al. 2005; Griffiths and Marquez 2007; Cheng et al. 2007; Zheng et al. 2009; Kupka et al. 2009; Fu and Liao 2010; Sternik 2013; Tschuchnigg et al. 2015; Ni et al. 2016; Sazzad and Moni 2017; Chatterjee and Krishna 2018) were performed for slope stability problems by using SRM. The literature review clearly indicates that the rigorous analysis for the two-layered cohesive-frictional soil slope is quite limited. Although a few stability studies (Kumar and Samui 2006; Sazzad et al. 2015; Sazzad and Moni 2017) were previously carried out by considering weaker layer overlying on strong layer, however, as per the findings, except the work of Sazzad et al. (2015), hardly any study seems to be available for the case where strong layer is considered to be placed over weak

stratum. The work of Sazzad et al. (2015) also pertains to a specific combination of layered system (Top Soil: c_1 = 10 kPa, ϕ_1 = 18° and Bottom Soil: c_2 = 6 kPa, ϕ_2 = 10°). Hence, there is a requirement to carry out an extensive and rigorous investigation to estimate the improvement in stability by placing a stronger layer over a weaker layer. This is the prime motivation to carry out the present work. In the present work, the factor of safety is estimated for different combinations of (i) slope geometry (i.e. slope angle, β), (ii) strength properties of the top (c_1, ϕ_1) and bottom layer (c_2, ϕ_2) (iii) and the thickness of the top layer (t). Furthermore, the effect of placing different stronger layers over the weaker bottom layers is thoroughly investigated.

5.2 STRENGTH REDUCTION METHOD (SRM)

The SRM is commonly used with the linear Mohr-Coulomb criterion, where the failure strength is characterized by cohesion (c) and the internal friction angle (ϕ). The Mohr-Coulomb model is expressed as follows:

$$\tau = c + \sigma_n \tan\phi \tag{5.1}$$

where, τ is the maximum amount of shear stress the soil can resist for a certain applied normal stress (σ_n). The analysis is carried out by reducing the strength parameters (c,ϕ) progressively until the slope becomes unstable. In conventional SRM, both parameters are reduced by the same factor, or in other words, the reduction path of the cohesion and the friction are identical. The reduced cohesion and the friction angle are computed from the following expression:

$$c_r = \frac{c}{F_s} \quad ; \qquad \tan\phi_r = \frac{\tan\phi}{F_s} \tag{5.2}$$

where, (i) c_r and ϕ_r are the reduced strength parameters, and (ii) F_s is the strength reduction factor. These reduced parameters are then reinserted into the model till the

failure occurs. The main objective of SRM approach is to compute the strength reduction factor and the reduced material parameters that lead to collapse state.

In the present analysis, Optum G2 (2018) is used for estimating the factor of safety of the slope through strength reduction method. OptumG2 is a finite element limit analysis (FELA) based software developed by OptumCE. For obtaining the limiting solutions, OptumG2 uses second order cone programming to solve the plane-strain stability problems. This scheme works by infeasibility detection in a very controllable way (Sloan 2011; Krabbenhoft and Lyamin 2015). Following steps are adopted for the formulation:

Step 1: Assuming F_{min} and F_{max}; where, F_{min} and F_{max} are the minimum and maximum value of factor of safety. Generally, F_{min} is chosen to be zero and F_{max} is taken to be a large number within the range of machine precision.

Step 2: Initializing the value of F_s and computing reduced strength parameters with the help of Eq. (5.2).

Step 3: Checking feasibility through the interior point method by using the reduced strength parameters.

Step 4: If the problem is feasible, assign $F_{min}=F_S$ and evaluate a new factor of safety by using the harmonic mean as depicted in Eq. (5.3).

$$F_s = \left[\frac{1}{2}\left(\frac{F_{\min} F_{\max}}{F_{\min} + F_{\max}}\right)\right] \tag{5.3}$$

Otherwise, if the problem is infeasible, assign $F_{max}=F_S$ and evaluate a new factor of safety by following the arithmetic mean as expressed in Eq. (5.4).

$$F_s = \frac{1}{2}\left(F_{\min} + F_{\max}\right) \tag{5.4}$$

Step 5: Continue the iterative process (Step 1–Step 4) until the following convergence condition as mentioned in Eq. (5.5) is fulfilled:

$$\frac{F_{\max} - F_{\min}}{F_s} < T_L \tag{5.5}$$

here, the tolerance limit, T_L, is kept as 0·01.

It is worth mentioning that based on the solution process, F_{min} and F_{max} provides the limiting extremities of the bound theorem. F_{min} and F_{max} represent rigorous lower and upper bound on the factor of safety corresponding to the statically admissible stress field domain and kinematically admissible velocity field domain, respectively. The numerical values presented herein are the average of both the limiting values.

5.3 PROBLEM STATEMENT AND METHODOLOGY

Fig. 5.1 shows a two-layered soil slope having an angle, β. The strength parameters of the top and the bottom layer are represented by c_1, ϕ_1, and c_2, ϕ_2, respectively. The soil plasticity is assumed to govern by the Mohr-Coulomb failure criterion and associated flow rule. The height of the slope (H), in the present analysis, is taken as 20 m for representing the high cut slopes. With the aid of the strength reduction method, it is intended to analyze and subsequently compute the factor of safety of three different two-layered slopes (namely, 25°, 35°, and 45°) made of different soil materials.

For performing the analysis, the size of the domain is considered adequately high so that the failure surface remains contained well within the domain. Based on trials, the height (D) and length (L) of the domain are kept as 2H and 9H, respectively. The boundary conditions are mentioned in Fig. 5.1. Vertical and horizontal displacements are restrained along the base of the considered domain. Along the left and right boundaries, horizontal displacement is not allowed to occur. The soil mass is discretized by using three nodded linear triangular elements. Adaptive mesh refinement based on plastic shear dissipation has been used. Three iterations of adaptive meshing

with 10,000 elements have been considered for all analyses. A nonlinear optimizer named sonic is used in Optum G2 software for optimization.

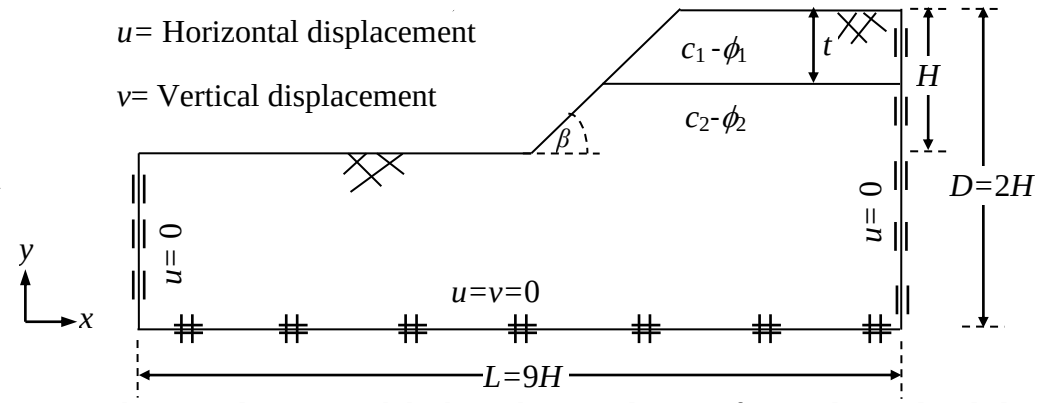

Fig. 5.1 Schematic diagram and the boundary conditions of a two-layered soil slope.

5.4 RESULTS AND DISCUSSIONS

In the present work, solutions are presented in terms of factor of safety for different combinations of the (a) slope angles (β), (b) soil strength properties of the top and the bottom layers (c_1, ϕ_1, and c_2, ϕ_2), and, (c) top layer thickness (t). Stability charts are presented in tabular form. Tables 5.1–5.3 show the factor of safety values computed for three different two-layered slopes (β= 25°, 35°, and 45°). The effect of placing different stronger layers over the weaker bottom layers is thoroughly investigated. The soil properties of both layers were widely varied in the analysis. In this study, nine different stronger soil layers [(35,0), (35,5), (35,8), (40,0), (40,5), (40,8), (45,0), (45,5), (45,8)] were considered to be placed over twelve different weaker bottom layer [(20,5), (20,10), (20,15), (20,20), (25,5), (25,10), (25,15), (25,20), (30,5), (30,10), (30,15), (30,20)]; the first and second part within the parenthesis indicate the frictional (in degrees) and cohesive strength (in kPa), respectively. The thickness of the stronger

Table 5.1 The proposed stability chart (indicating the factor of safety) corresponding to ϕ_2=20°.

ϕ_1	c_1 (kPa)	c_2 (kPa)	t=0.2D			t=0.4D			t=0.5D			t=0.6D			t=0.8D		
			β=25°	β=35°	β=45°	β=25°	β=35°	β=45°	β=25°	β=35°	β=45°	β=25°	β=35°	β=45°	β=25°	β=35°	β=45°
35°	0	5	1.074	0.782	0.603	1.224	0.903	0.683	1.354	0.996	0.675	1.504	1.001	0.694	1.504	1.001	0.694
		10	1.217	0.913	0.685	1.331	0.998	0.677	1.443	1.002	0.692	1.504	0.996	0.694	1.504	1.001	0.694
		15	1.345	1.004	0.685	1.428	1.002	0.674	1.504	1.002	0.674	1.504	0.996	0.694	1.504	0.996	0.694
		20	1.464	1.001	0.701	1.504	1.002	0.674	1.504	1.002	0.675	1.504	1.001	0.694	1.504	1.001	0.694
	5	5	1.101	0.811	0.634	1.278	0.974	0.774	1.411	1.126	0.930	1.740	1.298	0.980	1.816	1.298	0.980
		10	1.240	0.938	0.750	1.379	1.063	0.852	1.497	1.200	0.981	1.794	1.298	0.980	1.816	1.298	0.980
		15	1.365	1.049	0.851	1.475	1.143	0.921	1.577	1.264	0.981	1.821	1.298	0.980	1.816	1.298	0.980
		20	1.484	1.155	0.944	1.563	1.219	0.983	1.654	1.296	0.981	1.818	1.298	0.980	1.817	1.298	0.980
	8	5	1.114	0.827	0.649	1.306	1.007	0.812	1.438	1.162	0.978	1.777	1.409	1.084	1.943	1.409	1.084
		10	1.253	0.951	0.764	1.406	1.096	0.891	1.524	1.238	1.039	1.829	1.409	1.084	1.943	1.409	1.084
		15	1.376	1.062	0.864	1.500	1.175	0.958	1.604	1.304	1.082	1.880	1.409	1.084	1.943	1.409	1.084
		20	1.495	1.167	0.958	1.587	1.250	1.019	1.682	1.364	1.087	1.930	1.409	1.084	1.943	1.409	1.084
40°	0	5	1.091	0.796	0.615	1.282	0.959	0.732	1.455	1.152	0.841	1.803	1.194	0.828	1.803	1.199	0.831
		10	1.235	0.929	0.733	1.403	1.069	0.838	1.546	1.195	0.840	1.803	1.199	0.828	1.803	1.194	0.831
		15	1.364	1.045	0.838	1.502	1.157	0.840	1.633	1.198	0.841	1.803	1.194	0.831	1.803	1.200	0.831
		20	1.479	1.153	0.839	1.595	1.198	0.840	1.713	1.197	0.832	1.803	1.200	0.824	1.803	1.194	0.831
	5	5	1.114	0.822	0.641	1.334	1.028	0.821	1.499	1.214	1.020	1.888	1.514	1.138	2.132	1.515	1.138
		10	1.258	0.951	0.761	1.444	1.125	0.909	1.588	1.297	1.091	1.945	1.514	1.138	2.132	1.515	1.138
		15	1.383	1.064	0.864	1.541	1.211	0.984	1.674	1.372	1.138	2.003	1.514	1.138	2.132	1.515	1.138
		20	1.502	1.171	0.959	1.634	1.293	1.050	1.755	1.441	1.139	2.058	1.514	1.138	2.132	1.515	1.138
	8	5	1.128	0.837	0.658	1.363	1.058	0.857	1.523	1.245	1.060	1.919	1.631	1.247	2.269	1.632	1.247
		10	1.268	0.964	0.773	1.468	1.153	0.943	1.611	1.328	1.135	1.976	1.631	1.247	2.269	1.632	1.247
		15	1.394	1.077	0.877	1.562	1.239	1.018	1.697	1.403	1.197	2.034	1.631	1.247	2.269	1.632	1.247
		20	1.511	1.183	0.971	1.654	1.320	1.087	1.777	1.473	1.246	2.090	1.631	1.247	2.269	1.632	1.247
45°	0	5	1.105	0.807	0.624	1.328	1.001	0.784	1.545	1.246	0.997	1.983	1.420	0.988	2.148	1.428	0.991
		10	1.253	0.942	0.749	1.468	1.132	0.897	1.639	1.235	0.993	2.046	1.428	0.991	2.148	1.428	0.991
		15	1.382	1.061	0.856	1.570	1.227	0.982	1.728	1.352	0.960	2.107	1.428	0.991	2.148	1.428	0.988
		20	1.504	1.169	0.952	1.669	1.313	0.988	1.814	1.422	0.991	2.148	1.414	0.988	2.148	1.428	0.988
	5	5	1.124	0.831	0.647	1.382	1.065	0.858	1.581	1.296	1.104	2.025	1.762	1.318	2.505	1.762	1.318
		10	1.271	0.963	0.770	1.504	1.181	0.960	1.675	1.386	1.187	2.087	1.762	1.320	2.505	1.762	1.318
		15	1.400	1.078	0.875	1.607	1.273	1.044	1.764	1.463	1.258	2.155	1.762	1.318	2.505	1.762	1.318
		20	1.520	1.186	0.973	1.701	1.361	1.117	1.848	1.544	1.317	2.215	1.762	1.318	2.505	1.762	1.320
	8	5	1.136	0.843	0.660	1.408	1.099	0.893	1.602	1.323	1.137	2.057	1.838	1.433	2.641	1.885	1.433
		10	1.282	0.973	0.781	1.524	1.207	0.992	1.694	1.411	1.220	2.119	1.887	1.433	2.641	1.885	1.433
		15	1.409	1.091	0.886	1.623	1.298	1.073	1.782	1.493	1.294	2.182	1.885	1.433	2.641	1.885	1.433
		20	1.529	1.195	0.983	1.718	1.384	1.147	1.867	1.569	1.360	2.244	1.885	1.433	2.641	1.885	1.433

Table 5.2 The proposed stability chart (indicating the factor of safety) corresponding to ϕ_2=25°.

ϕ_1	c_1 (kPa)	c_2 (kPa)	t=0.2D			t=0.4D			t=0.5D			t=0.6D			t=0.8D		
			β=25°	β=35°	β=45°	β=25°	β=35°	β=45°	β=25°	β=35°	β=45°	β=25°	β=35°	β=45°	β=25°	β=35°	β=45°
35°	0	5	1.297	0.885	0.698	1.405	1.000	0.674	1.504	1.002	0.692	1.504	1.001	0.694	1.504	1.001	0.694
		10	1.448	1.003	0.685	1.507	1.002	0.674	1.504	1.002	0.674	1.504	1.001	0.694	1.504	1.001	0.694
		15	1.506	1.000	0.685	1.504	1.001	0.677	1.504	1.002	0.692	1.504	1.001	0.694	1.504	1.001	0.694
		20	1.506	1.000	0.695	1.507	0.998	0.700	1.504	1.002	0.691	1.504	1.001	0.694	1.504	1.001	0.694
	5	5	1.329	0.971	0.750	1.479	1.101	0.858	1.603	1.232	0.974	1.818	1.298	0.980	1.816	1.298	0.980
		10	1.477	1.100	0.870	1.579	1.185	0.931	1.682	1.287	0.983	1.818	1.298	0.980	1.816	1.298	0.980
		15	1.607	1.217	0.976	1.671	1.262	0.993	1.756	1.296	0.981	1.818	1.298	0.980	1.816	1.298	0.980
		20	1.731	1.326	1.074	1.759	1.333	1.026	1.824	1.296	0.981	1.818	1.298	0.980	1.816	1.298	0.980
	8	5	1.349	0.989	0.770	1.515	1.142	0.907	1.641	1.281	1.045	1.946	1.409	1.084	1.943	1.409	1.084
		10	1.492	1.115	0.886	1.613	1.227	0.977	1.721	1.347	1.080	1.944	1.409	1.084	1.943	1.409	1.084
		15	1.623	1.233	0.991	1.705	1.303	1.038	1.797	1.398	1.087	1.946	1.409	1.084	1.943	1.409	1.084
		20	1.746	1.340	1.089	1.791	1.374	1.098	1.868	1.406	1.085	1.946	1.409	1.084	1.943	1.409	1.084
40°	0	5	1.322	0.955	0.729	1.499	1.094	0.821	1.660	1.198	0.841	1.803	1.199	0.831	1.803	1.199	0.828
		10	1.473	1.093	0.839	1.613	1.191	0.835	1.751	1.197	0.840	1.803	1.200	0.840	1.803	1.200	0.832
		15	1.607	1.205	0.841	1.713	1.198	0.833	1.802	1.197	0.841	1.803	1.199	0.831	1.803	1.192	0.833
		20	1.734	1.200	0.841	1.802	1.198	0.839	1.803	1.199	0.840	1.803	1.199	0.828	1.803	1.200	0.832
	5	5	1.352	0.986	0.764	1.563	1.177	0.924	1.725	1.357	1.100	2.126	1.514	1.138	2.132	1.514	1.138
		10	1.498	1.120	0.886	1.667	1.269	1.003	1.811	1.430	1.139	2.138	1.514	1.138	2.132	1.515	1.138
		15	1.629	1.237	0.993	1.764	1.351	1.075	1.893	1.490	1.139	2.134	1.514	1.138	2.132	1.515	1.138
		20	1.754	1.350	1.092	1.856	1.428	1.139	1.970	1.512	1.140	2.134	1.514	1.138	2.132	1.515	1.138
	8	5	1.368	1.004	0.781	1.595	1.213	0.967	1.756	1.398	1.155	2.168	1.631	1.247	2.269	1.632	1.247
		10	1.512	1.137	0.902	1.696	1.305	1.046	1.842	1.472	1.215	2.215	1.631	1.247	2.269	1.632	1.247
		15	1.643	1.252	1.007	1.791	1.386	1.114	1.923	1.540	1.248	2.265	1.631	1.247	2.268	1.632	1.247
		20	1.766	1.360	1.107	1.884	1.464	1.181	2.000	1.597	1.247	2.269	1.631	1.247	2.268	1.633	1.247
45°	0	5	1.555	1.166	0.925	1.726	1.313	1.036	1.890	1.498	1.116	2.212	1.531	1.115	2.211	1.533	1.112
		10	1.496	1.111	0.872	1.703	1.283	0.990	1.880	1.430	0.991	2.148	1.428	0.991	2.148	1.428	0.988
		15	1.626	1.234	0.881	1.806	1.374	0.994	1.969	1.429	0.989	2.148	1.414	0.991	2.148	1.423	0.988
		20	1.756	1.346	0.994	1.901	1.431	0.998	2.051	1.425	0.989	2.148	1.428	0.991	2.148	1.414	0.988
	5	5	1.367	1.001	0.772	1.630	1.240	0.981	1.837	1.471	1.217	2.312	1.762	1.318	2.505	1.762	1.320
		10	1.519	1.137	0.901	1.749	1.344	1.073	1.929	1.553	1.286	2.367	1.762	1.318	2.505	1.762	1.320
		15	1.653	1.257	1.008	1.848	1.433	1.152	2.008	1.628	1.320	2.422	1.762	1.318	2.505	1.762	1.320
		20	1.777	1.368	1.110	1.943	1.516	1.220	2.096	1.697	1.320	2.476	1.762	1.318	2.505	1.762	1.320
	8	5	1.381	1.016	0.789	1.663	1.277	1.021	1.864	1.506	1.264	2.344	1.885	1.433	2.641	1.885	1.433
		10	1.532	1.151	0.914	1.776	1.376	1.110	1.953	1.587	1.336	2.394	1.885	1.433	2.641	1.885	1.433
		15	1.664	1.269	1.022	1.872	1.464	1.186	2.039	1.663	1.397	2.457	1.885	1.433	2.641	1.885	1.433
		20	1.787	1.381	1.122	1.967	1.547	1.257	2.121	1.733	1.433	2.511	1.885	1.433	2.641	1.885	1.433

Table 5.3 The proposed stability chart (indicating the factor of safety) corresponding to ϕ_2=30°

ϕ_1	c_1 (kPa)	c_2 (kPa)	t=0.2D			t=0.4D			t=0.5D			t=0.6D			t=0.8D		
			β=25°	β=35°	β=45°	β=25°	β=35°	β=45°	β=25°	β=35°	β=45°	β=25°	β=35°	β=45°	β=25°	β=35°	β=45°
35°	0	5	1.506	1.000	0.704	1.504	1.002	0.674	1.504	1.002	0.677	1.504	0.996	0.694	1.504	1.001	0.694
		10	1.506	1.000	0.689	1.504	1.000	0.700	1.504	1.002	0.674	1.504	1.001	0.694	1.504	1.001	0.694
		15	1.506	1.000	0.685	1.506	1.000	0.662	1.504	0.997	0.676	1.504	0.996	0.694	1.504	1.001	0.694
		20	1.506	1.000	0.704	1.506	1.001	0.677	1.504	1.002	0.677	1.504	1.001	0.694	1.504	1.001	0.694
	5	5	1.566	1.130	0.865	1.658	1.205	0.924	1.746	1.283	0.983	1.818	1.298	0.980	1.816	1.298	0.980
		10	1.718	1.267	0.990	1.754	1.283	0.991	1.812	1.296	0.983	1.818	1.298	0.980	1.816	1.298	0.980
		15	1.857	1.388	1.102	1.843	1.346	1.025	1.822	1.296	0.981	1.818	1.298	0.980	1.816	1.298	0.980
		20	1.987	1.502	1.204	1.876	1.344	1.026	1.822	1.296	0.981	1.818	1.298	0.980	1.816	1.298	0.980
	8	5	1.590	1.156	0.891	1.703	1.259	0.982	1.804	1.361	1.076	1.944	1.409	1.084	1.943	1.409	1.084
		10	1.738	1.289	1.010	1.798	1.336	1.048	1.874	1.398	1.087	1.944	1.409	1.084	1.943	1.409	1.084
		15	1.875	1.405	1.121	1.888	1.407	1.105	1.936	1.407	1.085	1.944	1.409	1.084	1.943	1.409	1.084
		20	2.002	1.520	1.221	1.972	1.475	1.146	1.946	1.407	1.085	1.944	1.409	1.084	1.943	1.409	1.084
40°	0	5	1.560	1.113	0.839	1.687	1.198	0.833	1.804	1.199	0.834	1.803	1.199	0.833	1.803	1.186	0.823
		10	1.717	1.199	0.839	1.800	1.198	0.829	1.805	1.200	0.829	1.803	1.200	0.831	1.803	1.192	0.840
		15	1.805	1.198	0.841	1.802	1.198	0.835	1.803	1.197	0.840	1.803	1.200	0.824	1.803	1.199	0.828
		20	1.805	1.205	0.841	1.802	1.198	0.833	1.806	1.197	0.834	1.803	1.192	0.831	1.803	1.192	0.831
	5	5	1.574	1.131	0.862	1.727	1.248	0.942	1.868	1.367	1.002	1.984	1.370	1.002	1.985	1.370	1.002
		10	1.731	1.273	0.991	1.832	1.337	1.022	1.941	1.368	1.003	1.984	1.370	1.003	1.985	1.370	1.002
		15	1.870	1.398	1.104	1.929	1.398	1.029	1.983	1.368	1.003	1.984	1.370	1.002	1.985	1.370	1.002
		20	2.002	1.510	1.139	2.015	1.398	1.029	1.983	1.368	1.003	1.984	1.370	1.003	1.984	1.370	1.002
	8	5	1.597	1.155	0.886	1.771	1.306	1.008	1.918	1.454	1.135	2.134	1.514	1.138	2.132	1.514	1.138
		10	1.749	1.291	1.010	1.872	1.391	1.081	1.999	1.507	1.139	2.134	1.514	1.138	2.132	1.514	1.138
		15	1.888	1.414	1.124	1.967	1.472	1.147	2.075	1.512	1.140	2.134	1.514	1.138	2.132	1.515	1.138
		20	2.017	1.527	1.226	2.058	1.543	1.188	2.140	1.514	1.140	2.134	1.514	1.138	2.132	1.515	1.138
45°	0	5	1.589	1.139	0.737	1.794	1.296	0.975	2.003	1.429	0.991	2.148	1.428	0.992	2.148	1.428	0.988
		10	1.748	1.283	0.990	1.921	1.411	0.992	2.091	1.425	1.001	2.148	1.428	0.988	2.148	1.428	0.988
		15	1.890	1.411	0.987	2.024	1.430	0.987	2.148	1.429	0.991	2.148	1.428	0.992	2.148	1.428	0.988
		20	2.022	1.428	0.987	2.120	1.427	0.988	2.148	1.429	0.996	2.148	1.428	0.988	2.148	1.428	0.988
	5	5	1.603	1.154	0.878	1.830	1.345	1.026	2.034	1.551	1.173	2.340	1.609	1.177	2.340	1.609	1.177
		10	1.760	1.297	1.011	1.946	1.444	1.113	2.120	1.610	1.175	2.340	1.609	1.177	2.340	1.609	1.177
		15	1.899	1.426	1.127	2.048	1.534	1.190	2.202	1.610	1.175	2.340	1.609	1.177	2.340	1.609	1.177
		20	2.029	1.541	1.233	2.145	1.612	1.203	2.280	1.610	1.175	2.340	1.609	1.177	2.340	1.609	1.177
	8	5	1.621	1.173	0.901	1.871	1.396	1.087	2.070	1.610	1.288	2.505	1.762	1.318	2.505	1.762	1.318
		10	1.777	1.314	1.029	1.984	1.491	1.170	2.157	1.683	1.320	2.504	1.762	1.318	2.505	1.762	1.318
		15	1.913	1.441	1.141	2.080	1.575	1.240	2.239	1.744	1.320	2.504	1.762	1.318	2.505	1.762	1.318
		20	2.043	1.553	1.249	2.177	1.655	1.309	2.319	1.759	1.319	2.504	1.762	1.318	2.505	1.762	1.318

layer was varied between 20%-80% of the domain height (i.e. t=0.2D, 0.4D, 0.5D, 0.6D, and 0.8D). Both the limiting values (lower and upper bounds) were obtained.

Therefore, a total number of 3240 [3 (number of slopes) x 9 (number of stronger layers) x 12 (number of weaker bottom layers) x 5 (number of variation of the thickness of the stronger layer) x 2 (number of limiting analysis i.e. lower and upper bounds)] computations were performed. Following observations and the subsequent inferences are made from the numerical results:

(a) The factor of safety (F_s) decreases with an increase in slope angle (β). However, this decrement depends on the strength of the soil layers. For an example, as β varies from 25° to 45°, F_s reduces markedly. This reduction differs by 14% (from 53 to 39%) as the cohesive strength of the top layer, (ϕ_1=35°, and, t/D=0.4) which is rested upon a certain bottom layer (c_2=20 kPa, ϕ_2=25°), increases up to 8 kPa from 0 kPa.

(b) Placing a stronger layer over a weaker stratum undoubtedly improves the stability of the slope and this improvement is more significant for steep slopes. For the previous example, (i) if the cohesive strength of the top layer rises from 0 to 8 kPa (keeping ϕ_1 equals to be 35°), the improvement in F_s for 25° and 45° slope occurs by 19% and 56%, respectively; and, (ii) if the frictional strength increases from 35° to 45°, F_s improves by 26% and 42% for 25° and 45° slope, respectively.

(c) When the thickness of the top layer is within a certain limit, the strength of the bottom layer also influences the stability of the slope. There is almost a linear relationship between the improvement of F_s with the increase in cohesive strength of the bottom layer. However, the relation between the improvement

of F_s with the increase in frictional strength of the bottom layer is highly nonlinear.

(d) The tabulated data clearly reveals that the improvement in F_s is quite significant as the top layer thickness changes from 0.2*D* to 0.4*D*. On the contrary, when *t/D* ratio varies from 0.6 to 0.8, the improvement in stability is almost negligible. The effect of the thickness of the top layer is further studied graphically.

Fig. 5.2 illustrates the variation of F_s with *t/D* for a 25° slope. Fig. 5.2a and 5.2b represent the cases where weaker bottom layer (ϕ_2=25°) is strengthened by placing two different cohesionless layer of friction angle 40° and 45°. Figs. 5.2c and 5.2d displays the cases where the cohesion of the top layer is considered as 8 kPa. It is quite evident that higher the strength of the top layer higher would be the safety factor, F_s. These figures depict that there is a certain *t/D* beyond which there is hardly any improvement in stability of the slopes. This particular top layer thickness is termed as optimum thickness and is referred here as dimensionless parameter, 't_{opt}/D'. The value of t_{opt}/D increases with the increase in the strength of the top layer. The figure shows that the dependence of t_{opt}/D on the cohesive strength of the bottom layer is further influenced by the frictional strength of the top layer; when ϕ_1=40°, t_{opt}/D decreases with increase in c_2, however, when ϕ_1=45° there is no impact of c_2 on the computed value of t_{opt}/D.

Fig. 5.3 shows the variation of F_s with *t/D* for β=25° and 45°, corresponding to two different ϕ_2, namely, 20° and 30°. The properties of the top layer are kept to be constant and the cohesive strength of the bottom layer is varied within the range of 5–20 kPa. The figures clearly reveal that for the same soil properties, optimum thickness of the top layer is significantly smaller for the steeper slopes. As the frictional strength of the bottom layer increases, the magnitude of t_{opt}/D further reduces. The numerical

solutions give an impression that the impact of the strength of the top layer on the stability is much higher than the strength of the bottom layer.

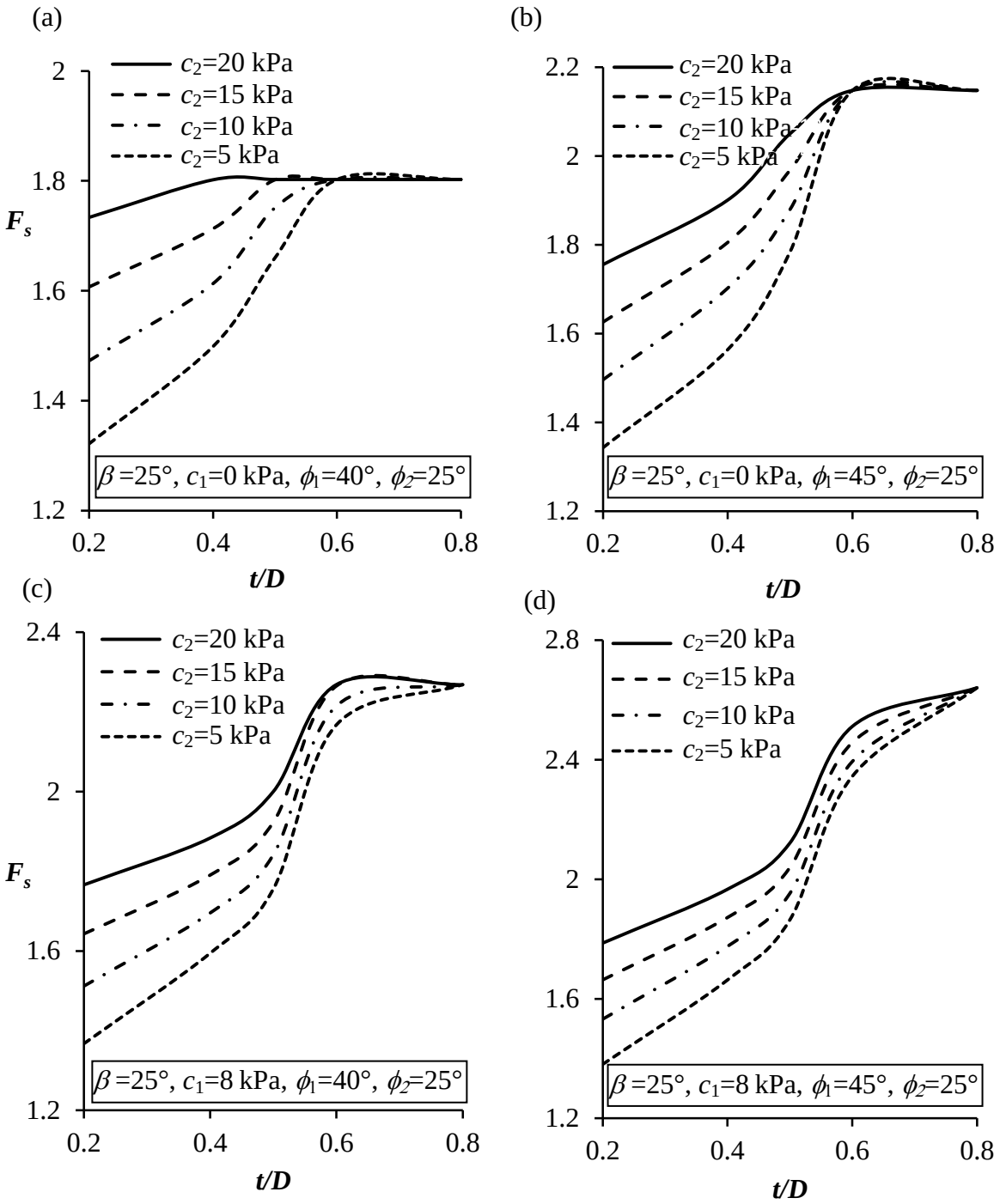

Fig. 5.2 The variation of F_s with t/D for a two-layered slope (β=25°) corresponding to varying c_2 and (a) c_1=0 kPa, ϕ_1=40°, ϕ_2=25°, (b) c_1=0 kPa, ϕ_1=45°, ϕ_2=25°, (c) c_1=8 kPa, ϕ_1=40°, ϕ_2=25° and (d) c_1=8 kPa, ϕ_1=45°, ϕ_2=25°.

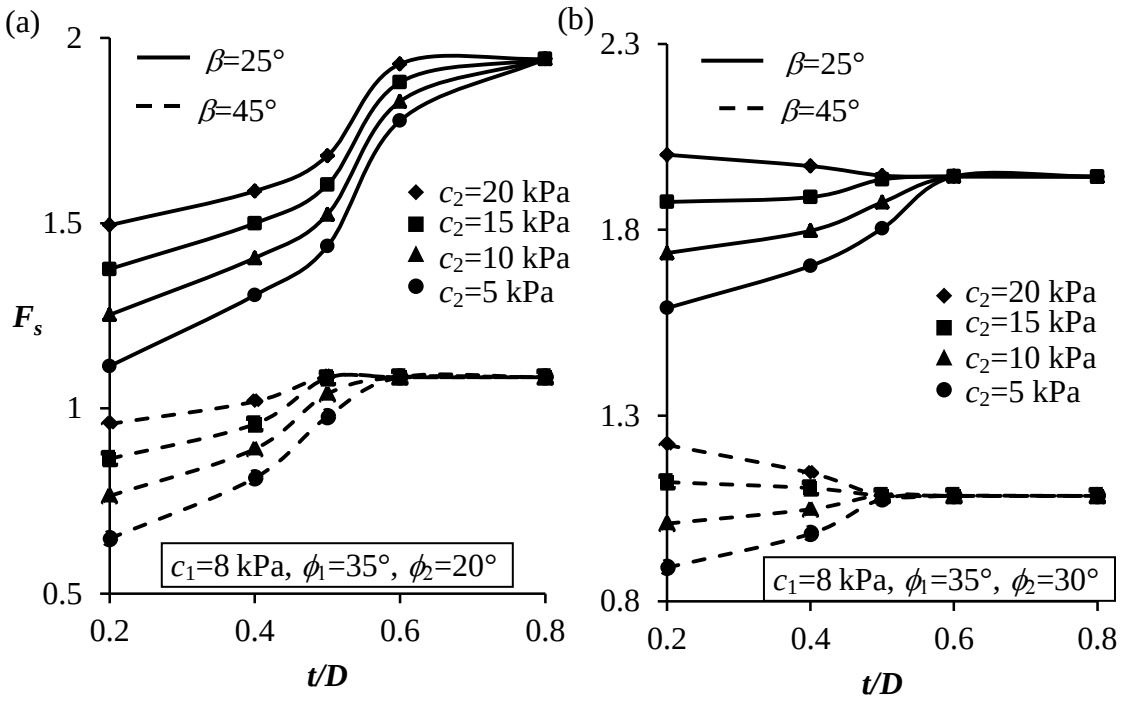

Fig. 5.3 The variation of F_s with t/D for two different layered slopes (β=25° and 45°) corresponding to varying c_2 and (a) c_1=8 kPa, ϕ_1=35°, ϕ_2=20° and (b) c_1=8 kPa, ϕ_1=35°, ϕ_2=30°.

Fig. 5.4 shows the mesh pattern at the collapse state for three different slope angles, namely, 25°, 35° and 45°. The soil profiles for these three cases are kept to be the same. It is to be noted that adaptive mesh refinement technique continuously updates the sizes of all the elements in an optimal fashion by computing the variations of stresses and velocities. Finer elements were automatically placed in the shear failure zone. Hence, these meshes indirectly depict the failure patterns. The figure shows that the size of the failure zone decreases with the increase in slope angle. Moreover, as the slope angle increases the failure is likely to become toe failure. This observation is in accordance with the studies of Lim et al. (2015) and Sazzad et al. (2015) who had earlier reported that if the top layer is considered to be stronger than the bottom layer and the slope angle is considered to be less than equal to 45° the incipient state of collapse in the soil slope will be triggered by developing base failure. As the steepness of the slope increases, the extent of the failure zone seems to be restricted closer to the slope surface.

Fig. 5.5 illustrates failure state corresponding to three different thickness of the top layer. The soil properties of the top layer as well as the bottom layer are the same for all the three cases. The figure demonstrates that as the thickness of the top layer increases the type of failure surface turns from toe to base. However, beyond a certain thickness, the slope collapses by developing the toe failure surface and the shear zone seems to be confined within the top layer. This observation substantiates the existence of t_{opt}/D.

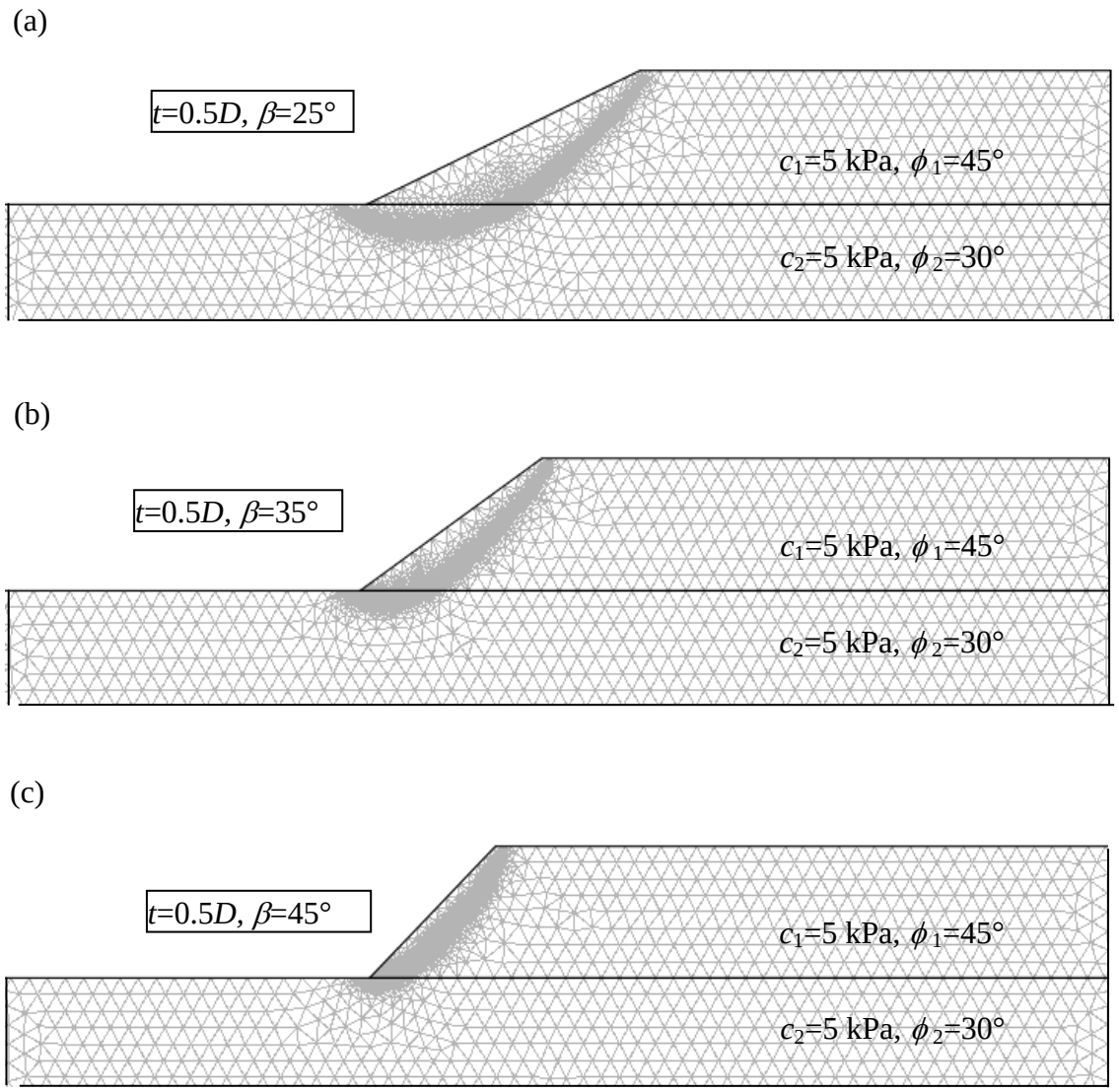

Fig. 5.4 Adaptive mesh patterns at the collapse state for three different slopes: (a) β=25°, (b) β=35° and (c) β=45°.

Fig. 5.6 depicts the mesh pattern at the collapse state corresponding to three different frictional angle of the top layer. All other geometrical and material strength parameters are kept to be the same. The figure illustrates that as the frictional strength of the top layer increases the failure zone grows in size. However, the extent at which the finer elements are laid at the collapse state goes thinner with the increase in ϕ_1. It gives an impression that the thickness of the shearing zone (i.e. shear band) becomes smaller with the placement of stronger layer over a weaker stratum.

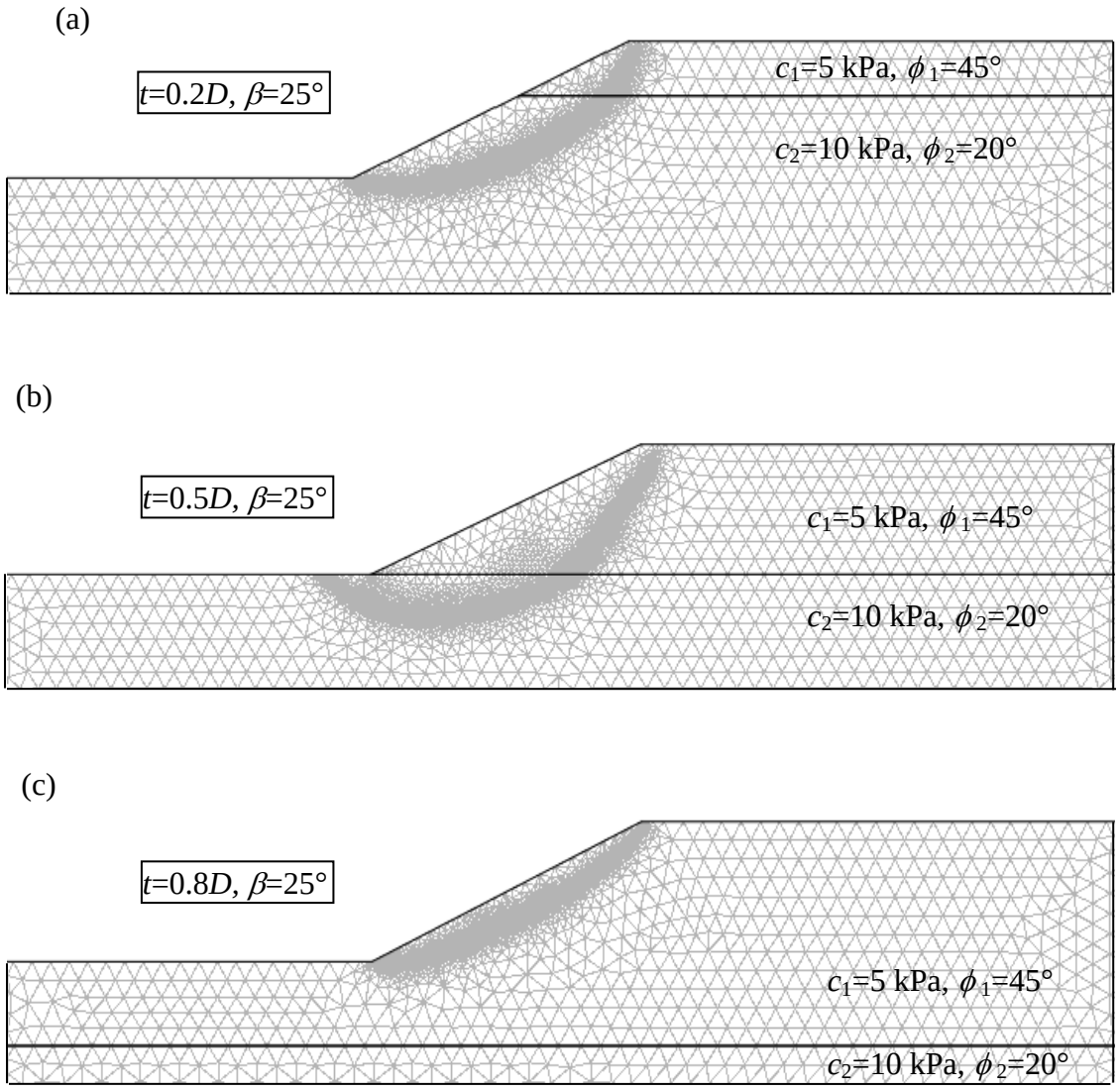

Fig. 5.5 Adaptive mesh patterns at the collapse state by varying the top layer thickness: (a) t=0.2D, (b) t=0.5D and (c) t=0.8D.

5.5 COMPARISON OF RESULTS

Comparisons of both the limiting solutions, for the homogenous and layered slopes, are presented in Tables 5.4 and 5.5, respectively. In most of the cases the difference seems to be in the second decimal place. Closeness of the lower and upper bound solutions further

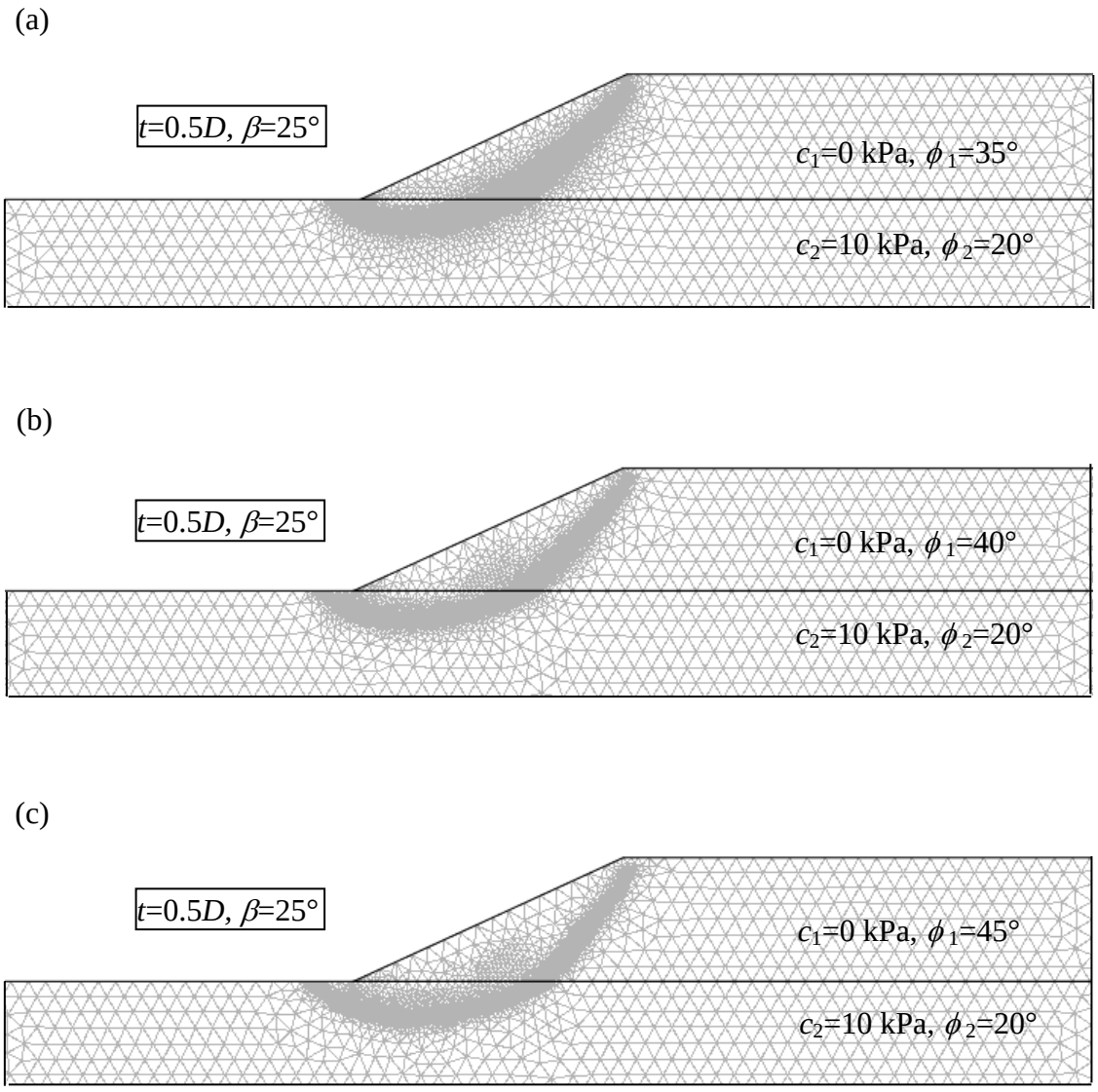

Fig. 5.6 Adaptive mesh patterns at the collapse state by varying the top layer frictional strength: (a) ϕ_1=35°, (b) ϕ_1=40°and (c) ϕ_1=45°.

depicts the accuracy in the computed solutions. Limit theorems suggest that the true solution will lie somewhere between these bounding values. It should be recalled that the safety factors charts presented in Tables 5.1, 5.2, 5.3, are the average value of the two extremities.

Table 5.4 A comparison of the computed lower and upper bound values of F_s for different homogeneous slopes

ϕ^*	c^{**} (kPa)	β=25°	β=35°	β=45°
25°	20	1.687 (1.695)	1.292 (1.303)	1.048 (1.058)
	15	1.560 (1.566)	1.177 (1.187)	0.940 (0.951)
	10	1.419 (1.425)	1.050 (1.060)	0.827 (0.831)
	5	1.258 (1.263)	0.904 (0.913)	0.692 (0.698)

Note: The values within and outside the parenthesis are obtained by using UB and LB method respectively.
*ϕ = internal friction angle of homogeneous soil slope.
**c= cohesion of homogeneous soil slope.

Table 5.6 shows the comparison of the present solutions computed with the numerical results provided by Dawson et al. (1999) for a homogenous slope of 10m height having unit weight of soil, γ=20 kN/m^3 and cohesion, c=12.38 kPa. Dawson et al. (1999) had employed the strength reduction method by using the explicit finite difference code, *FLAC*. As the frictional strength of the soil increases, the present method provides higher stability value. For the same soil, the difference between these two solutions reduces as the steepness of the slope increases. The reason may be attributed not only to the methodology but also to the choice of elements. Dawson et al. (1999) had discretized the chosen domain with four nodded rectangular elements, whereas, in the present work, three nodded linear triangular elements are used. The same trend is also observed while the solutions of Dawson et al. (1999) are compared

Table 5.5 A comparison of the computed lower and upper bound values of F_s for different layered slopes

ϕ_1	c_1 (kPa)	c_2 (kPa)	t=0.2D			t=0.5D			t=0.8D		
			β=25°	β=35°	β=45°	β=25°	β=35°	β=45°	β=25°	β=35°	β=45°
45°	5	5	1.121 (1.126)	0.828 (0.834)	0.644 (0.649)	1.577 (1.584)	1.293 (1.299)	1.101 (1.107)	2.495 (2.514)	1.754 (1.769)	1.312 (1.323)
		10	1.269 (1.273)	0.959 (0.966)	0.765 (0.774)	1.671 (1.678)	1.383 (1.389)	1.184 (1.189)	2.495 (2.514)	1.754 (1.769)	1.312 (1.323)
		15	1.397 (1.402)	1.074 (1.082)	0.869 (0.880)	1.760 (1.767)	1.456 (1.470)	1.255 (1.261)	2.495 (2.514)	1.754 (1.769)	1.312 (1.323)
		20	1.515 (1.525)	1.182 (1.189)	0.967 (0.978)	1.844 (1.851)	1.541 (1.547)	1.312 (1.322)	2.495 (2.514)	1.754 (1.769)	1.312 (1.328)

Note: The values within and outside the parenthesis are obtained by using UB and LB method respectively.

with the upper bound solutions (assuming log spiral mechanism) obtained by Chen (1975). It is to be noted that the present finite element limit solutions are quite smaller than those rigid block upper bound solutions provided by Chen (1975). It shows the improvement of the solutions when finite element limit analysis is employed for the analysis.

Table 5.6 A comparison of F_s obtained by Dawson et al. (1999) and Chen (1975) with the present solutions for homogeneous slopes of 10 m height

β (°)	ϕ (°)	Present study	Dawson et al. (1999)*	Chen (1975)**
15	5	0.932	1.023	0.890
	10	1.368	1.027	2.816
30	10	0.895	1.034	0.836
	15	1.111	1.027	1.343
	20	1.330	1.033	2.552
45	10	0.701	1.019	0.576
	20	0.994	1.026	1.000
	30	1.295	1.031	2.200
	40	1.645	1.008	5.482

*By using the explicit finite difference code, *FLAC*.
** By using rigid block method with an assumption of a continuous log-spiral failure mechanism.

Table 5.7 shows the comparison of the present solutions with the results provided by Kumar and Samui (2006) by using the rigid block upper bound method considering log-spiral failure mechanism. The comparison is carried out in terms of stability number for 45° slope corresponding to different soil layer properties and varying top layer thickness. Similar to the previous observation, it is well noted that the present solutions become quite smaller than the reported solutions of Kumar and Samui (2006) as the strength of the soil layer increases.

Table 5.8 illustrates the comparison of current solutions with the solutions provided by Chatterjee and Krishna (2018) for non-homogeneous slopes. Chatterjee and Krishna (2018) used (i) SLIDE v6 and Morgenstern and Price (1965) method for performing the LEM analysis and (ii) PHASE v9 for obtaining the FE solutions. The present solutions are quite agreeable with the reported FE solutions.

Table 5.7 A comparison of stability number obtained by Kumar and Samui (2006) with the present solutions in terms of stability number considering β=45° and c_1=c_2

		t=0.4H		t=0.6H	
ϕ_1 (°)	ϕ_2 (°)	Present study	Kumar and Samui (2006)*	Present study	Kumar and Samui (2006)
10	20	0.054	0.071	0.058	0.074
	30	0.043	0.050	0.055	0.059
	40	0.042	0.020	0.053	0.025
20	30	0.041	0.038	0.044	0.045
	40	0.034	0.014	0.041	0.017
30	40	0.032	0.012	0.034	0.013

* By using the rigid block upper bound method considering multi- log-spiral failure mechanism.

Table 5.8 A comparison of F_s obtained by Chatterjee and Krishna (2018) with the present solutions considering β=26.57°

				t=0.4D			t=0.5D			t=0.6D		
c_1 (kPa)	ϕ_1 (°)	c_2 (kPa)	ϕ_2 (°)	Present study	Chatterjee and Krishna (2018)		Present study	Chatterjee and Krishna (2018)		Present study	Chatterjee and Krishna (2018)	
					LEM-MP*	SRM**		LEM-MP	SRM		LEM-MP	SRM
10	30	0	36	1.46	1.747	1.65	1.57	1.790	1.66	1.67	1.790	1.69
		25	18	1.55	1.603	1.55	1.62	1.673	1.63	1.67	1.790	1.68
0	36	10	30	1.46	1.594	1.51	1.45	1.591	1.50	1.45	1.591	1.50
25	18			1.62	1.705	1.64	1.52	1.643	1.55	1.51	1.593	1.51

*LEM-MP- Limit equilibrium method (Morgenstern and Price)
**SRM- Strength reduction method

Table 5.9 depicts the comparison of present solutions with limit equilibrium solutions presented by Sazzad et al. (2015) for layered soil slopes. Sazzad et al. (2015) used Bishop Method (1955) for LEM analysis. The present solutions appear tobe smaller than the LEM solutions. This can be attributed to the fact that LEM solutions

generally overestimate the factor of safety due to the usage of statical and kinematical assumptions. This is also observed in earlier studies as well (Yu et al. 1998).

Table 5.9 A comparison of F_s obtained by Sazzad et al. (2015) with the present solutions considering $\phi_1 = \phi_2 = 0°$ and $\beta = 45°$

c_2/c_1	Present study	Sazzad et al. (2015)*
0.2	0.34	0.50
0.4	0.56	0.78
0.6	0.77	0.88
0.8	0.97	1.18
1.0	1.17	1.38
1.2	1.36	1.40
1.4	1.36	1.40
1.6	1.36	1.40
1.8	1.36	1.40

N.B: *By using LEM-Bishop Method (1955)

Table 5.10 demonstrates the comparison of present solutions obtained by employing SRM with results computed from the variational method for two layered slope problem which is depicted in chapter 3. The comparison is carried out for slope angle 45^o corresponding to top layer and bottom layer frictional angle 18^o and 30^o, respectively. The top layer thickness is considered as $t = 0.5H$. The solution obtained from the SRM shows significantly higher values compared to the outcomes derived from the variational approach. This gives an impression that the stability of the structure provided by the variational method is conservative in nature.

Table 5.10 A comparison of F_s obtained by the variational method with the present solutions (SRM) considering $\phi_1 = 18°$, $\phi_2 = 30°$, and $\beta = 45°$

c_1/c_2	Present study (SRM)	Variational method*
0.2	0.50	0.23
0.4	0.60	0.26
0.6	0.69	0.31
0.8	0.78	0.39

N:B: *By using Variational method (VM) as illustrated in Chapter 3

5.6 SUMMARY

In the present chapter, the stability of two-layered soil slopes is investigated by using the strength reduction method. A series of upper and lower bound limit analyses are carried out in Optum G2 software by placing different stronger layers of varied thickness over the weaker stratum. Stability charts are prepared in the form of the factor of safety for various soil properties, slope geometries, and top layer thickness. The amount of improvement in the stability by placing a layer of stronger soil over the weaker stratum is numerically investigated. The optimum thickness of the top layer is reported for a wide range of slopes. The extent and the type of failure zones are presented for several cases. The obtained solutions compared quite well with the available solutions. The proposed design charts provide a comprehensive overview of how slope stability is influenced by slope geometry, strength properties of layers, and layer thickness. This enhanced understanding allows engineers to make informed decisions during the design process, taking into account the interplay of various factors.

5.7 LIMITATIONS

The strength reduction method (SRM) typically exhibits insensitivity to variations in the dilation angle, stiffness parameters, or the size of the solution domain. The present method is mainly based on the frame work of finite element method (FEM) and hence, few shortcomings of FEM are retained in this method. The significant limitations of this method are the following: (i) the outcomes obtained from the method can be sensitive to the mesh density and the element type used, and (ii) accurate representation of boundary conditions is crucial for the method. Furthermore, it is crucial to recognize that the stability charts proposed in this study are applicable only to scenarios where a stronger soil layer is positioned above a weaker one.